Optical properties of polyvalent metals in the solid and liquid state: lead

1995 J. Phys.: Condens. Matter 7 907

(http://iopscience.iop.org/0953-8984/7/5/013)

J. Phys.: Condens. Matter 7 (1995) 907–918. Printed in the UK

Optical properties of polyvalent metals in the solid and liquid state: lead

Bernd Hüttner

German Aerospace Research Establishment (DLR), Institut für Technische Physik, Pfaffenwaldring 38–40, 70569 Stuttgart, Germany

Received 5 October 1994

Abstract. Recently we proposed a semiphenomenological theory for the calculation of the optical properties of polyvalent metals. In this paper, we apply it to the heavy metal lead and show that, in contrast to the preceding paper, no fitting parameter is basically necessary. The general agreement between experimental results and theoretical curves if satisfactory for all properties in both the solid and the liquid state. The optical properties in the liquid state are more similar to those of the solid state than to those of a free-electron system and therefore cannot be described by a simple Drude model.

1. Introduction

In our first paper relating to the optical properties of polyvalent metals we proposed a semiphenomenological theory for the calculation of the frequency and temperature dependence of all optical quantities and successfully applied it to aluminium (Hüttner 1994). We used this metal first because it is certainly the most investigated one. Consequently, it should be the best object for testing the model over a wide frequency and temperature range. Unfortunately, in the case of lead we are not able to compare all evaluated quantities with experimental data. Because of similar physical mechanisms in both metals, however, the general trend for lead should be correct and the quantities should at least have the right order of magnitude and be suited for use in other calculations, e.g. as input parameters for the determination of the temperature in laser heating.

Despite the fact that the band structure of the heavy metal lead is strongly influenced by relativistic effects (Jank and Hafner 1990, Kubo and Yamashita 1986) we can expect that, comparable to aluminium, the interband conductivity is dominated by the contribution of the parallel bands. Although several measurements show that the Fermi surface of lead possesses a nearly-free-electron character (Liljenvall *et al* 1970) the optical properties are far from showing Drude behaviour, at least for photon energies above about 1 eV. This is clearly due to the increasing influence of the interband effects with increasing photon energies.

The primary purpose of this paper is to investigate to what extent the deviations of the optical properties from the simple Drude model can be attributed to the transitions between parallel bands and to compare the results with experiments wherever possible.

The organization of this paper is as follows. In section 2, we give a brief summary of our semiphenomenological model with an extension of the former approach. We will not repeat all steps but refer to our preceding paper I (Hüttner 1994). An evaluation of the optical properties of lead in the solid and liquid phase is made in section 3. A discussion

0953-8984/95/050907+12$19.50

Table 1.

	Solid ($T = 300$ K)	Liquid ($T = 601$ K)
$\omega_{IB,1}$ (eV)	1.25[a]	1.0[a]
$\omega_{IB,2}$ (eV)	2.35[a]	1.4[a]
ω_p (eV)	13.0[b]	12.7[c]
ρ_{DC} ($\mu\Omega$ cm)	21.0[d]	95.0[e]
M	2.2[f]	1.3[a]
τ_{IB} (10^{-15} s)	0.64[g]	0.37[h]
ε_0	1.09[i]	1.2[i]
B	0.2[j]	0.2
β_{DC} ($\mu\Omega$ cm K^{-1})	0.093 $T_0 = 300$ K[k]	0.048[e]
β (K^{-1})	2.39×10^{-5} [l]	1.24×10^{-4} [e]

[a] Inagaki *et al* (1982).
[b] Raether (1980).
[c] Calculated by equations (12) and data from Iida and Guthrie (1993).
[d] Ashcroft and Mermin (1976).
[e] Iida and Guthrie (1993).
[f] Ashcroft and Lawrence (1968).
[g] Calculated by equation (10) and data from Mathewson and Myers (1971).
[h] Calculated by equations (10) and (12).
[i] Estimated, no values available.
[j] Golovashkin and Motulevich (1968).
[k] Fit to the data from Ashcroft and Mermin (1976) and Iida and Guthrie (1993).
[l] Touloukian (1975).

of the results and of some necessary modifications for lead in comparison with aluminium is given in section 4.

2. Theoretical model

It is well known that the knowledge of the complex frequency- and temperature-dependent conductivity $\sigma(\omega, T)$ is the basis for the calculation of the optical properties. In paper I we obtained the following expression for the complex conductivity

$$\sigma(\omega, T) = \sigma_D(\omega, T) + \sigma_{IB}(\omega, T) \tag{1}$$

where

$$\sigma_D(\omega, T) = \sigma_{DC}/(1 - i\omega\tau_D(T)) \tag{2}$$

is the Drude (nearly-free-electron) part and

$$\sigma_{IB}(\omega, T) = -i\frac{\omega_p^2(T)\omega}{4\pi}\sum_n \frac{A_n}{\omega_n^2 - (\omega + i/\tau_{IB,n}(T))^2} \tag{3}$$

represents the interband contribution derived in paper I for parallel bands.

For the reader's convenience, we repeat the relation between the complex conductivity and the complex dielectric function commonly used in the calculation of the optical properties

$$\varepsilon(\omega, T) = \varepsilon_0 + i4\pi\sigma(\omega, T)/\omega. \tag{4}$$

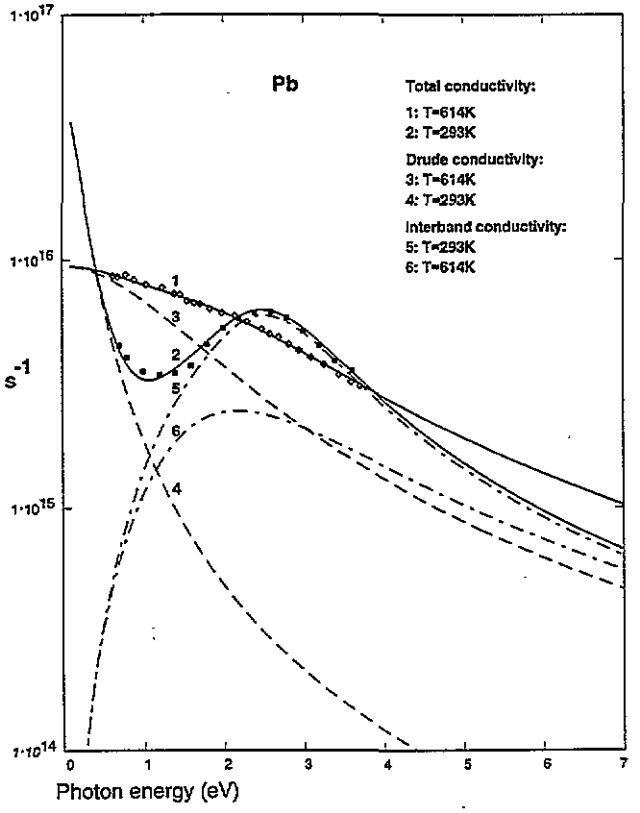

Figure 1. A semilogarithmic plot of the real part of the total (solid line), the Drude (dashed line) and the interband conductivity (dash–dotted line) in CGS units. The experimental values are taken from Mathewson and Myers (1971) (■) and Inagaki *et al* (1982) (◊).

The symbols in equations (2) and (3) have the following meanings. The DC conductivity is given by

$$\sigma_{DC}(T) = -\omega_p^2 \tau_D(T)/4\pi M = \Omega_p^2 \tau_D(T)/4\pi \tag{5a}$$

where ω_p is the plasma frequency as measured by electron-scattering experiments, Ω_p is the plasma frequency of nearly free electrons, and $m^* = Mm$ is the effective electron mass with m as the bare electron mass.

$\tau_p(T)$ represents the temperature-dependent Drude relaxation time taken from experiment. For the energy difference belonging to the nth parallel bands in the interband term we have set

$$\omega_n = \omega_{lm} = \hbar^{-1}(E_l(k) - E_m(k)) \qquad E_m(k) \leqslant E_F \leqslant E_l(k) \tag{5b}$$

with E_F denoting the Fermi energy level and ω the photon energy. Further,

$$A_n = (2/m\hbar\omega_n)\langle p_{lm}^2 \rangle \tag{5c}$$

is an average oscillator strength and $\tau_{IB,n}(T)$ is an interband scattering time. It is shown below that this relaxation time can be calculated in the framework of the theory and is therefore, in contrast to paper I, not a free parameter, at least in principle.

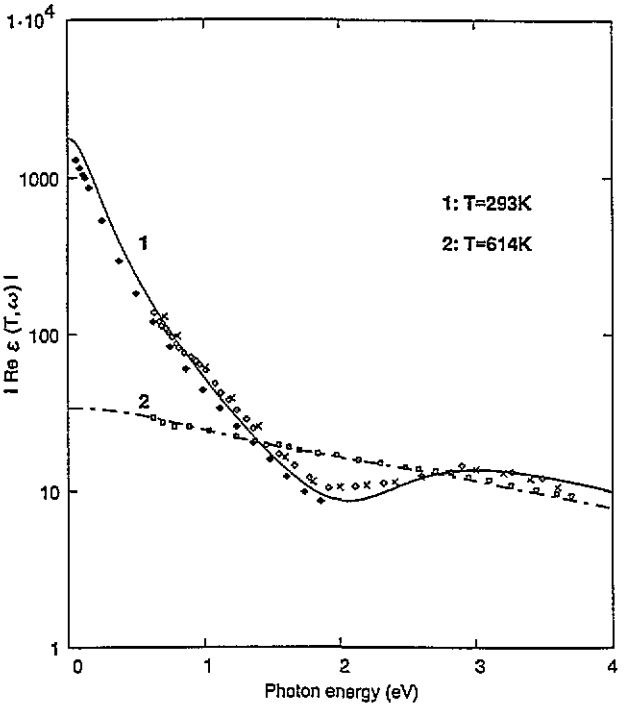

Figure 2. The absolute value of the real part of the dielectric function at $T = 293$ K (solid line) and $T = 614$ K (dash–dotted line). Data points are from Liljenvall *et al* (1970) (◇), Ordal *et al* (1987) (♦), Mathewson and Myers (1971) (×) and Inagaki *et al* (1982) (□).

Some authors showed (for example Brust (1970) and Smith and Shiles (1978)) that the sum of the oscillator strengths is related to the effective mass by the sum rule

$$\sum_n A_n = \varepsilon_0 - 1/M. \tag{6}$$

In formula (6) we have replaced 1 by the more general expression ε_0 that is connected with the polarization α of the rest of the crystal by $\varepsilon_0 = 1 + \alpha$. In general, α is not a constant but it is expected that it has a low dispersion because in most cases d electrons or core electrons are lying deep enough below the Fermi energy. For aluminium we could set $\alpha = 0$ since the L states are about 70 eV below the Fermi edge. This is not so for lead, where the binding energies of the shallow d band are of the same order, around 17 eV below E_F (Jezequel *et al* 1977), as the plasmon energy. Consequently, an interaction between the dynamic response of the core and the valence electrons appears and α will be greater than zero (Sturm *et al* 1990).

The values for the single-oscillator-strength terms can be calculated from the ratio of the real parts of the interband conductivity taken at the maxima

$$A_n(T)/A_{n+1}(T) = [\mathrm{Re}\,\sigma_{\mathrm{IB}}(\omega_{\mathrm{max},n}, T)]/[\mathrm{Re}\,\sigma_{\mathrm{IB}}(\omega_{\mathrm{max},n+1}, T)]. \tag{7}$$

More details are given in paper I.

As mentioned above, the interband scattering time is available from the real part of the interband conductivity using the experimental data. For example, if two bands dominate the interband conductivity we obtain for the interband scattering time of the first transition

$$\tau_{\mathrm{IB},1}(T) = 8\pi\,\mathrm{Re}\,\sigma_{\mathrm{IB}}(\omega_{\mathrm{max},1}, T)(1 + B(T))/\omega_{\mathrm{p}}^2(T)(\varepsilon_0 - M(T)^{-1})B(T) \tag{8}$$

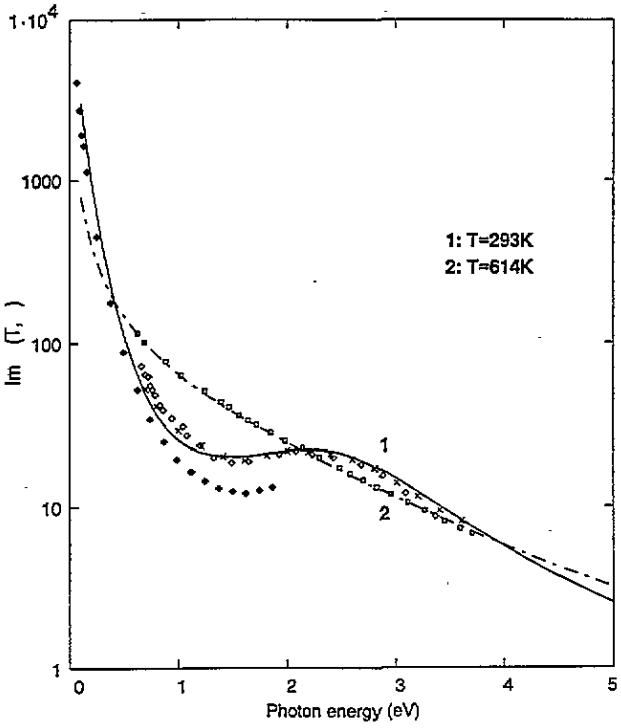

Figure 3. The imaginary part of the dielectric function at $T = 293$ K (solid line) and $T = 614$ K (dash–dotted line). Data points are from Liljenvall *et al* (1970) (◇), Ordal *et al* (1987) (♦), Mathewson and Myers (1971) (×) and Inagaki *et al* (1982) (□).

and for the second one

$$\tau_{IB,2}(T) = 8\pi \operatorname{Re}\sigma_{IB}(\omega_{max,2}, T)(1 + B(T))/\omega_p^2(T)(\varepsilon_0 - M(T)^{-1}) \tag{9}$$

where ω_{max} is the frequency at the maximum of the real part of the interband conductivity and $B(T)$ is given by the ratio of the amplitudes of $\operatorname{Re}\sigma_{IB}(T, \omega_{max})$ (equation (7)). These equations are obtained by taking the first derivative of the real part of the interband conductivity and solving the expressions for τ_{IB}.

In a first approximation, we can split the inverse relaxation times $\tau_{IB}(T)^{-1}$ into a temperature-independent part τ_{IB}^{-1} representing the strong electron–electron scattering above the Fermi surface and the usual electron–phonon scattering $\tau_D(T)^{-1}$ (Smith and Segall 1986)

$$1/\tau_{IB}(T) = 1/\tau_{IB} + 1/\tau_D(T). \tag{10}$$

Equation (10) is a useful relation because a numerical calculation of τ_{IB} is a tremendous task. One has to know the complete band structure and then one has to perform time-consuming averagings. To our knowledge this procedure has not been carried out yet.

For the temperature dependence of the DC conductivity in both solid and liquid state, we use, as in paper I, a linear approximation according to which

$$\rho_{DC}(T) = \rho_{DC}(T_0) + \beta_{DC}(T - T_0) \tag{11}$$

where the values are taken from experiment. All other quantities, such as the interband energies, the effective mass and the plasma frequency, are dependent on the volume. Since

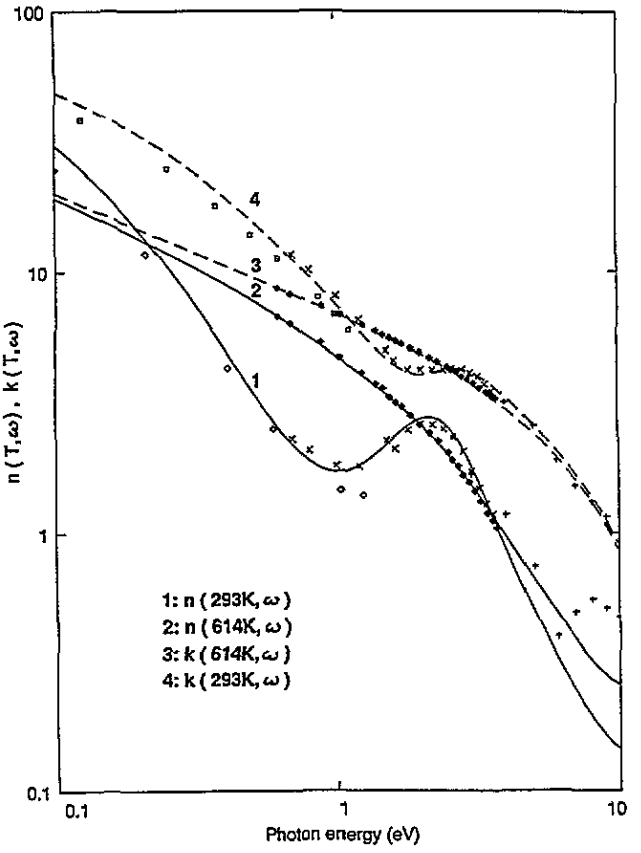

Figure 4. The refractive index (solid lines) and extinction coefficient (dashed lines) at $T = 293$ K (curves 1 and 4) and at $T = 614$ K (curves 2 and 3). Experimental points in the solid state are from Golovashkin and Motulevich (1968) (◇), Mathewson and Myers (1971) (×), Ordal et al (1987) (□) and Lemonnier et al (1973) (+) and those in the liquid state are from Inagaki et al (1982) (♦).

lead has a very small Debye temperature, 88 K (Ashcroft and Mermin 1976), and because we are not interested in the low-temperature behaviour we can describe the volume expansion by means of the linear thermal expansion coefficient. A general expression reads

$$f(V) = f(V_0)(V_0/V) \tag{12a}$$

where the volume V is given by

$$V(T) = V_0(1 + \beta_{s,l}(T - T_0)) \tag{12b}$$

with the volume expansion coefficient $\beta_{s,l}$ where s refers to the solid state and l to the liquid one, and T_0 an arbitrary reference temperature. Additional to this smooth behaviour, we have to keep in mind the change of density or atomic volume in the phase transition.

3. The optical properties of solid and liquid lead

In table 1, we have compiled all quantities that are used for the evaluation of the optical properties.

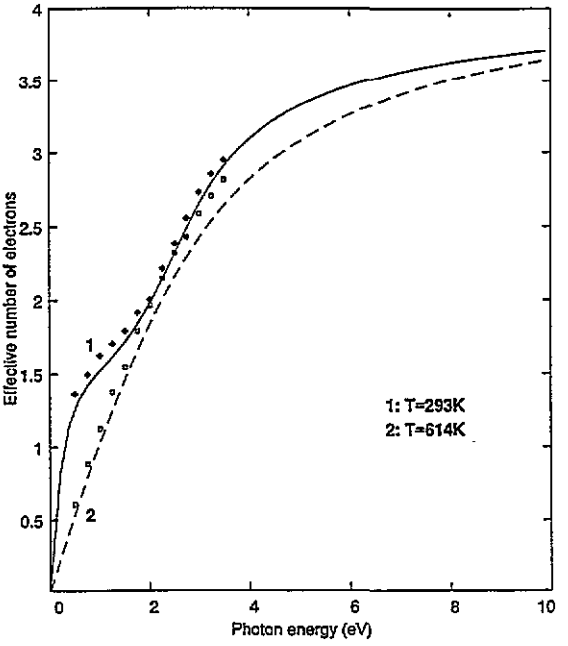

Figure 5. The effective number of electrons at $T = 293$ K (solid line) and $T = 614$ K (dashed line). Data points are taken from Inagaki *et al* (1982): $T = 293$ K (◇) and $T = 614$ K (□).

The real part of the total, Drude and interband conductivity, evaluated from equation (1), is plotted in figure 1 together with the experimental results (Mathewson and Myers 1971, Inagaki *et al* 1982). As expected, the total conductivity (curve 2) possesses a large maximum near 2.3 eV due to the contribution of the second interband transition. It is worth noting for the solid state that the Drude conductivity (curve 4) has lost its low-energy importance already in the energy range around 1 eV and that for energies above 2 eV it is more than one order of magnitude smaller than the interband contribution.

The peak of the first transition at 1.25 eV is completely masked by the larger contribution of the second one, primarily due to its wide broadening, which is related to the short relaxation time and to some extent to the small value of B. We will come back to this point in section 4.

In the liquid state, the total conductivity (curve 1) shows no structure. From such a featureless shape, it has been often concluded that interband transitions are completely absent and that liquid metals for this reason can be described by a free-electron model (Faber 1972, Shimoji 1977, Arakawa *et al* 1980). A comparison of curve 3 (Drude conductivity) with curve 6 (interband contribution) shows unambiguously that this assumption is wrong. On the contrary, for photon energies above 3 eV the interband contribution (curve 6) is even larger than the Drude part. Such a non-free-electron behaviour has been reported also in other properties. The electronic DOS of liquid lead, e.g., is found to be more similar to the shape of the solid metal than to the free-electron system. In pseudopotential calculations, this was theoretically confirmed by Jank and Hafner (1990) and experimentally by photoelectron spectroscopy by Indlekofer *et al* (1990). Their observations and our calculations allow the conclusion that the electronic structure of polyvalent metals is more sensitive to the local atomic potentials, which are hardly affected by the transition from the ordered to a disordered phase, than to the loss of periodicity that occurs upon melting.

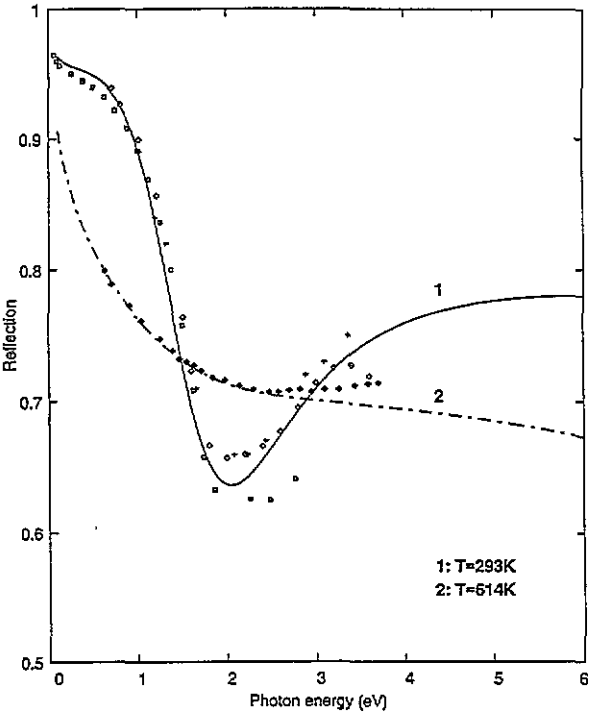

Figure 6. The reflectivity at $T = 293$ K (solid line) and $T = 614$ K (dash–dotted line). Data points are from Ordal *et al* (1987) (□), Mathewson and Myers (1971) (◇), Liljenvall *et al* (1970) (+) and Inagaki *et al* (1982) (♦).

In figures 2 and 3, the real and imaginary parts, respectively, of the dielectric function are plotted for both the solid ($T = 293$ K) and liquid ($T = 614$ K) states. As can be seen, the theoretical curves are in better agreement with the measurements of Liljenvall *et al* (1970) and Mathewson and Myers (1971) than with the more modern work of Ordal *et al* (1987). Two factors, we believe, may be the cause for the discrepancies. First, the samples were measured by Ordal *et al* (1987) under a pressure of ~ 0.04 Torr at ambient temperature. Under such conditions, contaminations appear, which give rise to a decrease of the absolute values with increasing frequencies but without essential alterations of the general shape (Liljenvall *et al* 1970). Second, ε_1 and ε_2 from Ordal *et al* (1987) have been evaluated from the surface resistance by a Kramers–Kronig analysis. For the calculation, they used the results of Golovashkin and Motulevich (1968), which were not measured under UHV conditions and assumed a smooth behaviour of the resistance above some electronvolts by omitting the large contributions to the optical conductivity due to the transitions from d levels into the conduction band for $\omega > 18$ eV (Jezequel *et al* 1977).

The refractive index, $n(\omega) = \sqrt{\mathrm{Re}\,\varepsilon(\omega)}$, and the extinction coefficient, $k(\omega) = \sqrt{\mathrm{Im}\,\varepsilon(\omega)}$, are presented for $\omega = (0.1\text{–}10)$ eV in figure 4. The general agreement is satisfying and the small deviations (Golovashkin and Motulevich (1968) and Ordal *et al* (1987)) are probabvly related to surface contaminations as discussed above. At high energies, the n and k values are obtained by a Kramers–Kronig analysis from reflectance data (Lemonnier *et al* 1973) and the authors suggest that the peak can be attributed to a normal interband transition between two K bands. Although this assumption is not perfectly established by photoemission, we will not discuss this point further, since our interest is

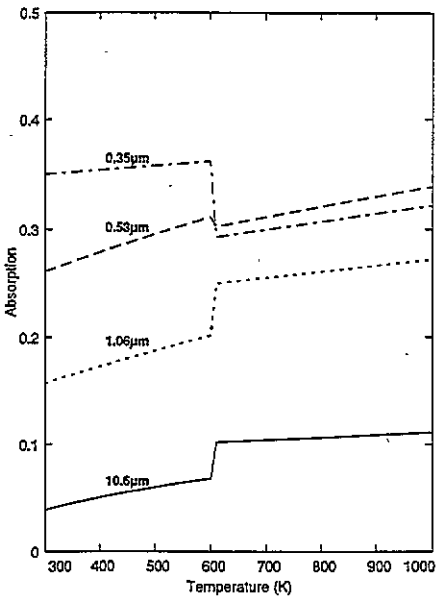

Figure 7. Absorption at four wavelengths: solid line, 10.6 μm; dotted line, 1.06 μm; dashed line, 0.53 μm and dash–dotted line, 0.35 μm.

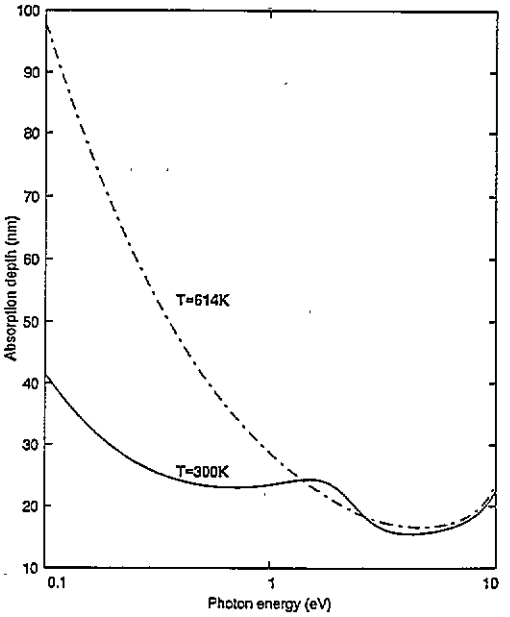

Figure 8. The optical absorption length at $T = 300$ K (solid line) and $T = 614$ K (dash–dotted line).

restricted on the one hand to the conbtribution of parallel bands and on the other hand to the range of available laser frequencies.

The frequency dependence of the effective number of electrons contributing to the optical conductivity is calculated from

$$n_{\mathrm{eff}}(\omega, T) = \frac{2m}{\pi e^2 N_{\mathrm{a}}(T)} \int_0^{\omega} \mathrm{Re}\,\sigma(\omega', T)\,\mathrm{d}\omega' \tag{13}$$

and plotted in figure 5. N_{a} represents the number of atoms per unit volume and e is the elementary charge.

Two points are remarkable, the large similarity between the two curves and the slow increase of $n_{\mathrm{eff}}(\omega)$.

In the remaining part of section 3, the absorption and reflection, respectively, of solid and liquid lead are investigated. Figure 6 displays a plot of the frequency dependence of the reflection and the available experimental results. The close agreement between the values of Ordal *et al* (1987) and Mathewson and Myers (1971) at low energies and the discrepancies appearing at higher energies confirm our conjecture on the influence of surface contamination. Obviously, the scattering of the experimental data at the end of the measurement ranges requires an extension to higher energies for a determination of the correct behaviour. The temperature dependence of the absorption for four often-used laser frequencies is given in figure 7. Common to all curves is the slow increase of the absorption with increasing temperature in both states but a strong wavelength-dependent change at the melting point. The different directions of the change are attributed to a competition between the enhancement of the absorption caused by the decreasing scattering time at T_{m} and the frequency-dependent shrinking of the interband contributions at the phase transition.

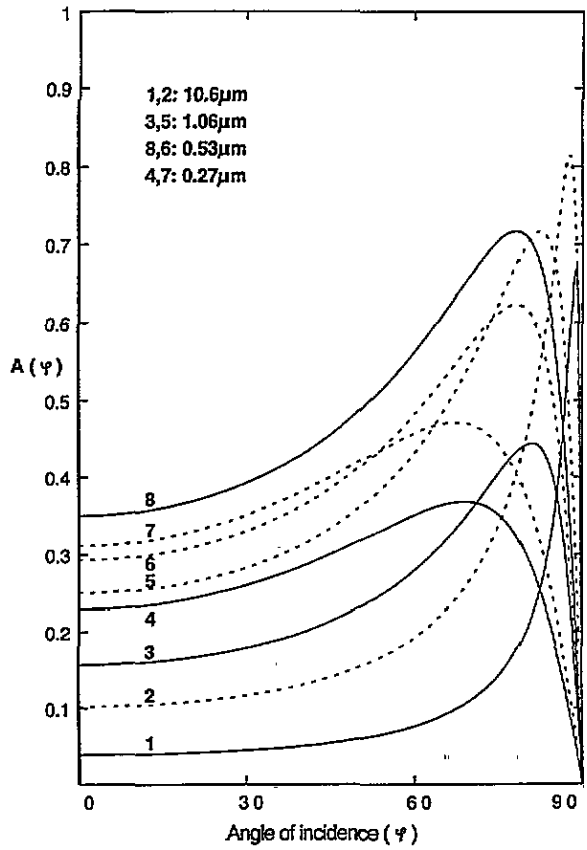

Figure 9. The absorption as a function of the angle of incidence at $T = 300$ K (solid curves) and at $T = 614$ K (dotted curves) for four wavelengths: 10.6 μm (1, 2), 1.06 μm (3, 5), 0.53 μm (8, 6) and 0.27 μm (4, 7).

Another parameter, the absorption length, especially important for the thermal stress under laser treatment, is plotted in figure 8. While an enhancement of the optical absorption length of roughly twofold exists between room temperature and the liquid state at long wavelengths, e.g. for a CO_2 laser, it is nearly unaffected at frequencies above 1 eV, e.g. Nd:YAG-laser frequencies.

So far, we have calculated all quantities for a normal incidence of light. In our last two figures, we display the angular dependence of the absorption (figure 9) and of the absorbed power density (figure 10). The curves are evaluated from the values of the complex refractive index as obtained from insertion into the usual expression for the angle dependence (see e.g. Heavens 1991). Because of the strong increase of the absorption up to the pseudo-Brewster angle, the absorbed power density, even for very short wavelengths, is nearly constant over a surprisingly wide range of angles of incidence. Only a small variation of the pseudo-Brewster angle is recognizable as a function of temperature but with frequency-dependent signs.

4. Discussion

The existence of parallel bands and the assumption that these predominantly contribute to the

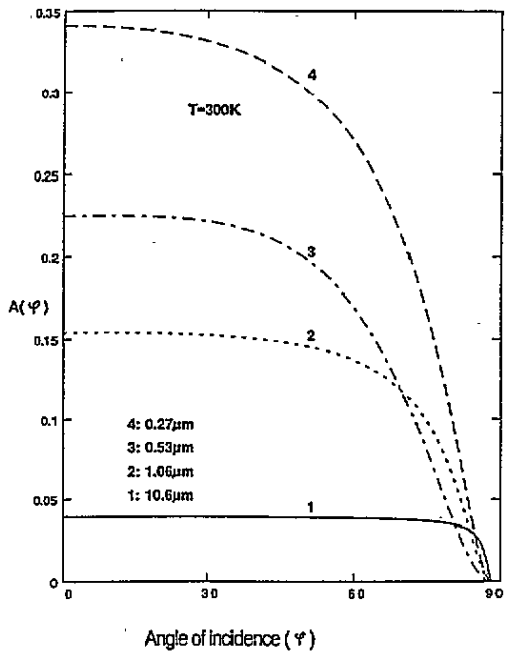

Figure 10. The absorbed power density as a function of the angle of incidence at $T = 300$ K for four wavelengths.

optical interband conductivity are the main conditions for the applicability of the proposed model. Inspection of band-structure calculations can confirm the first point and the second is supported by the large joint density of states due to the vanishing of the difference of the k gradients in the energy denominator, $\nabla_k(E_l(k) - E_m(k))$, for parallel bands. The amount of the omitted remaining interband contributions cannot, of course, be checked directly by such a simple semiphenomenological approach. Intensive and time-consuming calculations for every temperature would be necessary, as worked out, for example, by Sturm and Ashcroft (1974) for aluminium at a fixed temperature. As an indirect confirmation, we can take the agreement between the theoretical curves and the experimental results.

No values are available in the literature regarding the polarizability of solid and liquid lead. Therefore, we have chosen for the solid state a number lying in the range of the theoretically determined values for other polyvalent metals (Sturm *et al* 1990). In the liquid state, the enlarged value for the polarizability, necessary for an agreement with the experiments, could be explained by the decrease of the binding energies leading to stronger interactions between the core and conduction electrons. This is comparable to the reduction of the transition energies due to the dilation of the unit cell with increasing temperature.

A smaller value of the ratio of the real parts of the interband conductivity, 0.2 instead of 0.37 as determined by Golovashkin and Motulevich (1968), is used in the calculations. The wavelength-dependent influence of the contaminations, as discussed above, justifies the correction. Despite the good agreement between the theoretical curves and the experimental results in the liquid state, we will, before concluding this section, discuss some limitations of the model. Our starting equations are based on the Bloch–Boltzmann theory, which is valid as long as the mean free path is much longer than the interatomic spacing. Of all polyvalent metals, lead is the first candidate for violating this requirement. Specifically, it has the smallest Debye temperature, one of the largest electron–phonon coupling constants

and therefore a short scattering time (Allen *et al* 1986). Even if it is hard to say how many times longer the mean free path has to be than the atomic distance, the τ_{IB} (614 K) from table 1 corresponds to a mean scattering length of less than 10 Å, which should be, at least, at the limit of the validity of the Bloch–Boltzmann theory.

Concluding, we will add two remarks. First, the restriction to the contribution of parallel bands to the optical conductivity, by omitting all other possible interband transitions, leads to relatively simple equations, which can describe, however, in an astonishingly good manner the experimental results. Second, the optical and electronic properties of the liquid state of the heavy metal lead cannot, similarly to the light metal aluminium, be explained by a simple free-electron model (Drude theory). Since analogous results are to be expected for other polyvalent metals, perhaps, moreover, for all liquid metals, we have to recognize once again that it is not the loss of periodicity in the phase transition but the local atomic arrangements that is primarily decisive for the electronic properties of liquid metals.

References

Allen P B, Beaulac T P, Khan F S, Butler W H, Pinski F J and Swihart J C 1986 *Phys. Rev.* B **34** 4331
Arakawa E T, Inagaki T and Williams M W 1980 *Surf. Sci.* **96** 248
Ashcroft N W and Lawrence W E 1968 *Phys. Rev.* **175** 938
Ashcroft N W and Mermin N D 1976 *Solid State Physics* (Philadelphia, PA: Saunders)
Brust D 1970 *Phys. Rev.* B **2** 818
Faber T E 1972 *An Introduction to the Theory of Liquid Metals* (Cambridge: Cambridge University Press)
Golovashkin A I and Motulevich G P 1968 *Sov. Phys.–JETP* **26** 881
Heavens O S 1991 *Optical Properties of Thin Solid Films* (New York: Dover) p 51
Hüttner B 1994 *J. Phys.: Condens. Matter* **6** 2459
Iida T and Guthrie R I L 1993 *The Physical Properties of Liquid Metals* (Oxford: Oxford University Press)
Inagaki T, Arakawa E T, Caters A R and Glastad K A 1982 *Phys. Rev.* B **25** 6130
Indlekofer G, Pflugi A, Oelhafen P, Chauveau D, Guillot C and Lecante J 1990 *J. Non-Cryst. Solids* **117/118** 351
Jank W and Hafner J 1990 *Phys. Rev.* B **41** 1497
Jezequel G, Thomas J and Lemonnier J C 1977 *Solid State Commun.* **23** 559
Kubo Y and Yamashita J 1986 *J. Phys. F: Met. Phys.* **16** 2017
Lemonnier J C, Priol M and Robin S 1973 *Phys. Rev.* B **8** 5452
Liljenvall H G, Mathewson A G and Myers H P 1970 *Phil. Mag.* **22** 243
Mathewson A G and Myers H P 1971 *Phys. Scr.* **4** 291
Ordal M A, Bell R J, Alexander R W, Long L L and Querry M R 1987 *Appl. Opt.* **26** 744
Raether H 1980 *Excitations of Plasmons and Interband Transitions by Electrons (Springer Tracts in Modern Physics 88)* (Berlin: Springer)
Shimoji M 1977 *Liquid Metals* (London: Academic)
Smith D Y and Segall B 1986 *Phys. Rev.* B **34** 5191
Smith D Y and Shiles B 1978 *Phys. Rev.* B **17** 4689
Sturm K and Ashcroft N W 1974 *Phys. Rev.* B **10** 1343
Sturm K, Zaremba E and Nuroh K 1990 *Phys. Rev.* **42** 6973
Touloukian Y (ed) 1975 *Thermophysical Properties of Matter* vol 11 (New York: IFI/Plenum)